

Single-photon loading of polar molecules into an optical trap

Bart J. Schellenberg,^{1,2} Eifion H. Prinsen,^{1,2} Janko Nauta,³ Lukáš F. Pašteka,^{1,2,4} Anastasia Borschevsky,^{1,2} and Steven Hoekstra^{1,2,*}

¹*Van Swinderen Institute for Particle Physics and Gravity, University of Groningen, Groningen, The Netherlands*

²*Nikhef, National Institute for Subatomic Physics, Amsterdam, The Netherlands*

³*Experimental Physics Department, CERN, Geneva, Switzerland*

⁴*Department of Physical and Theoretical Chemistry, Comenius University, Bratislava, Slovakia*
(Dated: July 24, 2025)

We propose a scheme to transfer molecules from a slow beam into an optical trap using only a single photon absorption and emission cycle. The efficiency of such a scheme is numerically explored for BaF using realistic experimental parameters. The technique makes use of the state-dependent potential in an external electric field to trap molecules from an initial velocity of order 10 m/s. A rapid optical transition at the point where the molecules come to a standstill in the electric field potential irreversibly transfers them into a ~ 7 mK optical dipole trap. For a pulsed Stark decelerated beam, we estimated the per-shot efficiency to be $\sim 0.04\%$ or up to $\sim 10^3$ molecules, with a potential factor 20 improvement when the fields are synchronously modulated with the arriving velocity components. The irreversibility of the scheme allows for larger numbers to be built up over time. Since this scheme does not rely on a closed cycling transition for laser cooling, it broadens the range of molecules that can be used for research on cold molecular chemistry, quantum information, and fundamental interactions in optical traps.

I. INTRODUCTION

Trapped molecules are versatile systems that enable studies in many fields [1] such as cold molecular chemistry [2–7], quantum information processing [8, 9], and fundamental interactions [10, 11]. An optical trap is particularly attractive as it can trap molecules in states independent of their Stark or Zeeman shifts. Especially when operated at so-called magic conditions, where the ac-Stark shifts of two levels of interest are tuned to be the same, it offers an environment highly suitable for precision measurements. Although successful laser cooling [12–22] and magneto-optical trapping [13, 16, 23–30] have been demonstrated for a number of diatomic and polyatomic species, further cooling and compression is required to transfer molecules into an optical trap. In particular polyatomic molecules, consisting of three or more atoms, offer additional opportunities compared to diatomic systems due to their rich internal structures [31–34], while the complexity of their energy levels brings increased challenges for cooling. This primarily stems from the need to scatter a large number of photons without significant losses from the optical cycle, as well as the ability to sufficiently compress the molecule cloud.

In this work we propose a single-photon loading scheme with the purpose of directly transferring molecules from a slow beam into an optical trap. The scheme combines the state-dependent energy landscape in an externally applied electric field with an irreversible electronic transfer at a point where the kinetic energy of the molecule is minimized. Similar experiments using magnetic fields were previously designed [35–37] and

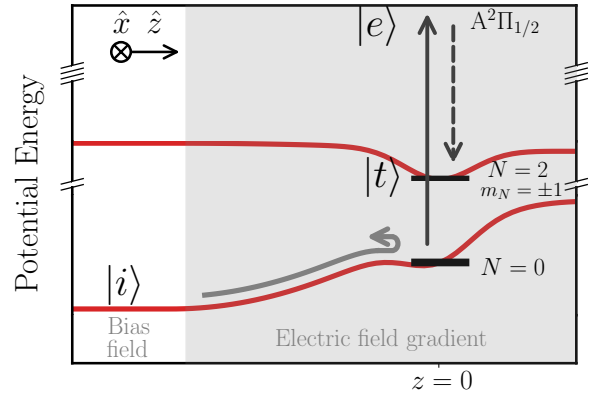


FIG. 1: A schematic of the single-photon loading scheme. Molecules approach from the left whilst in some initial state $|i\rangle$ and fly along the $+\hat{z}$ axis. At their turning point in the potential, they are pumped to an excited state $|e\rangle$, from which there is a chance to decay to the trapped state $|t\rangle$. The center of the optical trap is located at $z = 0$. A fraction of the molecules remain trapped in this state by the optical dipole trap.

performed [38–40] for both atoms and molecules. We numerically explore the efficiency of this process for the BaF molecule, as a prototype molecule that is interesting for precision experiments [41–44].

The central idea is illustrated in Figure 1. We start by preparing the molecules in the initial rotational state $|i\rangle = |0; 0\rangle$ (notation $|N; m_N\rangle$) of the $X^2\Sigma^+ v = 0$ vibronic ground state. This state has a relatively strong coupling to the external electric field through its Stark shift (see Figure 2a), which is favorable for molecules with a greater initial velocity. The molecules initially travel

* s.hoekstra@rug.nl

along the $+\hat{z}$ direction and into a repulsive potential that is formed using a negative electric field gradient. (That is, we apply a bias electric field to the molecules and have them travel away from this bias.) At the classical turning point inside the potential (i.e. where the molecules have minimal kinetic energy), we place an optical dipole trap using the standing-wave light field at 1064 nm inside an enhancement cavity. Once the molecules reach this optical trap, we electronically excite them to the short-lived excited state $|e\rangle = |J = 3/2; -\rangle$ in the $A^2\Pi$ $v = 0$ manifold, after which they promptly decay back to the $X^2\Sigma^+$ ground state. A portion of the molecules will decay to the $|t\rangle = |2; \pm 1\rangle$ rotational trapped state, whose Stark curve remains relatively unchanged by the external field (see Figure 2a), effectively disabling the electric field gradient for these molecules. The intermediate excited state $|e\rangle$ is chosen such that a laser driving the $|i\rangle \rightarrow |e\rangle$ transition does not also resonate with $|t\rangle$. This means that the scheme represents a one-way barrier, or "molecule diode". Successful loading occurs when the post-transition energy of the molecules is below the state-dependent depth of the optical trap.

II. MOLECULAR INTERACTIONS

The Stark curves for the lower lying rotational states of the electronic ground state of BaF are shown in Figure 2a. These curves were calculated by PGopher [45] using molecular constants from Rysiewicz *et al.* [46] and Ernst *et al.* [47]. In this analysis we neglect the hyperfine structure. The interaction of the molecules with the external electrostatic field is described by $H^{\text{Stark}} = -\mu_e \cdot \mathbf{E}$ (with μ_e being the electric dipole moment of BaF and \mathbf{E} the external field), and its interaction with the optical field by $H^{\text{opt}} = -\mathbf{d}_e \cdot \mathcal{E}$ (where \mathbf{d}_e represents the dipole operator and \mathcal{E} the electric component of the optical field.) When H^{Stark} remains sufficiently small compared to the rotational splitting, H^{opt} can be expanded into spherical tensor components [48, 49]

$$\begin{aligned} H_{ij}^{\text{opt}} &= -\frac{\mathcal{E}_0^2}{4} \sum_{k=0}^2 \mathcal{A}^k(\alpha(\omega)) \cdot \mathcal{P}^k(\hat{\mathcal{E}}, \hat{\mathcal{E}}^*), \\ &= -\frac{\mathcal{E}_0^2}{4} \left(\delta_{ij} \alpha^S(\hat{\mathcal{E}} \cdot \hat{\mathcal{E}}^*) + \right. \\ &\quad \left. + \epsilon_{ijk} \alpha_k^V(\hat{\mathcal{E}} \times \hat{\mathcal{E}}^*)_k + \alpha_{ij}^T(\hat{\mathcal{E}} \otimes \hat{\mathcal{E}}^*)_{ij} \right), \end{aligned} \quad (1)$$

where \mathcal{A}^k and \mathcal{P}^k are spherical tensors of rank k , taking into account the molecular polarizability and optical polarization respectively. The contributions of the scalar (α^S), vector (α^V), and tensor (α^T) components of the polarizability have been made explicit with the second equality. Summation over k is assumed, δ_{ij} represents the Kronecker delta, ϵ_{ijk} is the Levi-Civita symbol, and α_{ij}^T is a symmetric traceless operator. When the light is linearly polarized, the unit vector $\hat{\mathcal{E}}$ is real and

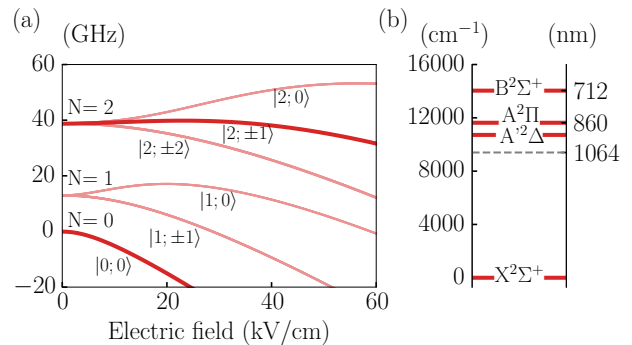


FIG. 2: a) The Stark curves of the lowest rotational levels (notation $|N; m_N\rangle$) in the $X^2\Sigma^+$ $v = 0$ vibronic state of BaF; b) The lowest electronic states in BaF. The dashed line indicates the wavelength used for the optical trap.

the vector term vanishes. The scalar component is isotropic and consequently independent of the molecular projection states. The tensor part is state-dependent and can introduce deviations from isotropy at the order of 10%. For an explicit derivation of the relevant operators, the reader is referred to the work by Caldwell *et al.* [49]. We found that whilst the introduction of the tensor polarizability can affect the trap depth at the order of 10%, it does not significantly impact the loading efficiency. This is because the molecules that are successfully transferred into the trap predominantly possess energies near the trapping threshold, which follows from the inevitable gain in momentum due to the attractive forces of the dipole trap.

		$\omega = 0$	$\omega = c/1064 \text{ nm}$
α_{\parallel}	$X^2\Sigma$	169.82(77)	288
	$A^2\Pi_{1/2}$	137.4(5.2)	-27
	$A^2\Pi_{3/2}$	136.3(3.1)	
α_{\perp}	$X^2\Sigma$	277.8(1.4)	671
	$A^2\Pi_{1/2}$	-1275(184)	-382
	$A^2\Pi_{3/2}$	-910(104)	

TABLE I: Parallel (α_{\parallel}) and perpendicular (α_{\perp}) static and dynamic polarizabilities of BaF in atomic units. At $\omega = c/1064 \text{ nm}$, the components for $X^2\Sigma$ differ from $\omega = 0$ primarily through coupling to the $A^2\Pi$ (α_{\perp}) and $B^2\Sigma$ (α_{\parallel}) states, and for $A^2\Pi$ by $X^2\Sigma$ (α_{\perp}) and $C^2\Pi$ (α_{\parallel}).

To determine the optical trap depth and the corresponding optical intensity that is required, we have calculated the polarizability of the molecule in the involved electronic states. The static polarizability of BaF in the $X^2\Sigma$, $A^2\Pi_{1/2}$, and $A^2\Pi_{3/2}$ states was calculated using the finite-field procedure based on the energies obtained by the DIRAC23 program package [50, 51] using the Fock-space coupled cluster method [52] and an exact 2-component Hamiltonian [53]. Augmented valence Dyall basis sets [54, 55] were used in the calcu-

lations. Cardinality and augmentation were increased until further refinements improved the polarizability at the order of only a few percent. The final results were calculated using the t-aug-dyall.v4z basis set. Similarly, various other computational parameters (level of theory, coupled cluster active space, relativistic Hamiltonians) were investigated. Based on this study, we assigned the theoretical uncertainties to the calculated values.

The dynamic polarizability was calculated at the coupled cluster (CCSD) level using the linear response method as implemented in the CFOUR program package [56, 57]. Relativistic effects were incorporated by use of Dunning’s pseudopotential basis sets [58–60], with an effective core potential on the barium atom, replacing its 46 innermost electrons. The final results were calculated using the aug-cc-pV5Z-PP basis set. Note that this scalar relativistic scheme does not account for spin-orbit splitting, and thus only yields the polarizability for the $A^2\Pi$ state as a whole. A summary of the relevant quantities is given in Table I. The details of the computational study are presented in the upcoming theoretical paper [61].

III. PARAMETERS

Within the context of this work we have selected to use a $\lambda = 1064$ nm trapping laser, as this wavelength is well red-detuned from the lowest electronic transition and intense lasers with good intensity and frequency stability are readily available at this wavelength. The intensity of the trapping laser is enhanced using a power build-up cavity to provide a sufficiently deep optical trap. When the separation of the cavity mirrors is large compared to the beam waist w_0 , the optical field of the trap reduces to that of a Gaussian standing wave. The resulting 1D lattice trap has an amplitude \mathcal{E}_0 that can be obtained from the incident laser power P and the cavity finesse \mathcal{F} through

$$\mathcal{E}_0 = \sqrt{\frac{4P\mathcal{F}}{\pi^2 w_0^2 c \epsilon_0}}, \quad (2)$$

which follows from integrating its transverse profile. In the absence of the external electric field, using equation (2) with (1) allows us to directly connect the trap depth with the configurable parameters P , w_0 , and \mathcal{F} . For instance, by coupling $P = 20$ W into a low finesse cavity of $\mathcal{F} = 500$ and $w_0 = 150$ μm , a 10 mK deep trap can be formed. The trap is oriented along the \hat{x} direction, which lies orthogonal to the molecular beam. Its potential takes the form of many closely-spaced discs, sometimes also referred to as ‘pancakes’. Each disc has a size of $dx \sim 0.5$ μm and $dy, dz \sim 100$ μm . It is to be noted that in the presence of the electric field, the combination of the AC and DC Stark shift skews the potential, which slightly reduces the actual depth. For our example, we

numerically computed an effective trap depth of about 7.3 mK for the above-mentioned configuration.

To optimize the shape of the electric potential for the loading scheme, we consider the difference between the electrostatic field at the position of the dipole trap and the upstream electric field to determine the height of the initial barrier in $|i\rangle$. We also optimize the slope of the electric field at the trap, which determines the trap depth in $|i\rangle$. For an idealized configuration, a steep slope is preferred as this prevents the molecules from regaining momentum when they enter the optical field. At the same time, the height of the initial barrier in $|i\rangle$ is tuned to match the initial energy of the incoming molecules, such that they come to a standstill close to the dipole trap.

The maximum capture velocity is determined by the shape of the Stark curve. For instance, by using an increasing electric field with $+\hat{z}$, molecules from the low-field-seeking $|i\rangle = |1; 0\rangle$ state can be brought to a standstill if their initial velocity was no greater than 4.5 m/s, before they reach their high-field-seeking regime beyond 19 kV/cm. Alternatively, molecules in the $|i\rangle = |2; 0\rangle$ state from up to 8.5 m/s can be stopped, but at the cost of requiring a much larger electric field (56 kV/cm). In order to capture molecules from a larger initial velocity using a more readily achievable electric field, whilst also providing a suitable candidate for $|t\rangle$, we found it better to reverse the situation. That is, one can use a decreasing electric field with $+\hat{z}$ to slow down molecules in a high-field-seeking state. Whilst the transverse stability for HFS states is a point of attention, deceleration under similar conditions has been achieved before [62, 63]. A loading scheme involving HFSs can be achieved using $|i\rangle = |0; 0\rangle$ and $|t\rangle = |2; \pm 1\rangle$ (see also Figure 2a). Starting at 40 kV/cm, these molecules can be stopped from up to 14 m/s. In the same electric field range, the $|t\rangle = |2; \pm 1\rangle$ level remains mostly unaffected. Since both states have a positive parity, and the transitions happen in a relatively weak electric field, which reduces state-mixing, they can be directly coupled using an intermediate state $|e\rangle$ of negative parity.

IV. LOADING

Having identified the most important parameters of the loading scheme, let us discuss the efficiency with which incoming molecules can be transferred into the optical trap. The above-mentioned trap depth of 7.3 mK corresponds to at most 0.88 m/s in kinetic energy, whilst the typical timescales involved in the electronic transitions range between tens to hundreds of nanoseconds [64, 65]. This means that during the optical transitions, the molecule does not move significantly inside the micrometer-sized trap, and we may consider the transfer $|i\rangle \rightarrow |e\rangle$ and subsequent decay $|e\rangle \rightarrow |t\rangle$ as an instantaneous process. This allows us to determine for each point in position-velocity phase space whether an instan-

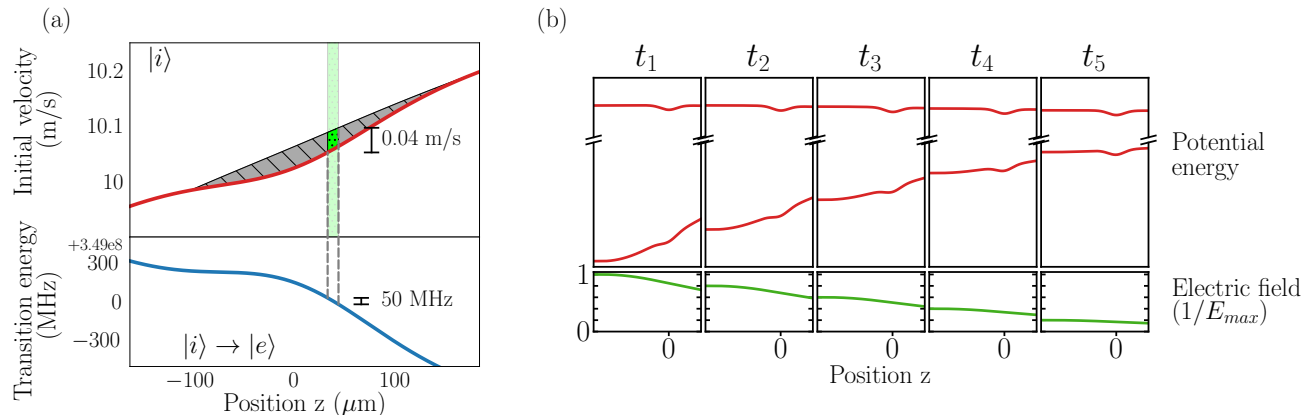


FIG. 3: *a) Top: phase space acceptance of molecules arriving in $|i\rangle$ into the trapped state $|t\rangle$. The solid red curve represents the potential following the AC and DC Stark effects, and effectively shows the position z where molecules with a given initial velocity will come to a standstill. Bottom: position-dependent transition energy for $|i\rangle \rightarrow |e\rangle$. Further details are elaborated in the main text; b) (Not to scale.) Modulating the external fields with time allows different velocity components to be captured, as the relative height of the trap in $|i\rangle$ decreases.*

taneous transfer at that point can move the molecule to inside the final optical potential of state $|t\rangle$. The corresponding phase space along (z, v_z) is shown in the upper half of Figure 3a, indicated by the gray shaded (striped) areas.

The next step is to consider the conditions under which a resonant excitation $|i\rangle \rightarrow |e\rangle$ can be driven. Since the differential Stark shift in the electric and optical fields depends on the position of the molecule, the linewidth of the excitation can be up to a few hundred MHz, as is indicated by the lower half of Figure 3a. This means that a laser source with a large linewidth is preferred. Using an optical modulator, we intend to broaden the pump light such that molecules within a 50 MHz linewidth can be excited. The green shaded (dotted) area in Figure 3a illustrates the part of the phase space where the excitation energy lies within a 50 MHz bandwidth and where the molecules can be successfully transferred for this particular example. At the same time, it is important to ensure that no transitions involving the already trapped molecules in $|t\rangle$ lie within the same bandwidth. For our case, we choose $|e\rangle = |J = 3/2; -\rangle$ of the $A^2\Pi_{1/2}$ $v = 0$ manifold, such that the excitation energy is sufficiently far detuned from any transition involving $|t\rangle$. The lifetime of the $A^2\Pi_{1/2}$ states in BaF is 57.1(3) ns [65], and the branching ratios to $|i\rangle = |0; 0\rangle$ and $|t\rangle = |2; \pm 1\rangle$ in $X^2\Sigma^+$ $v = 0$ are 67% and 25% respectively [66]. By rapidly re-exciting the molecules between $|i\rangle$ and $|e\rangle$ until they decay to $|t\rangle$, we can thus transfer at best $\frac{0.25}{1-0.67} \approx 75\%$ to $|t\rangle$.

The efficiency with which molecules can be transferred into the optical trap depends on the matching of the trap and electric field parameters with the properties of the incident molecular beam. As an example, let us consider a Stark decelerated molecular beam [41], whose molecules travel at a longitudinal velocity of $v_z = (10 \pm 1)$ m/s, within a $dx, dy = 1$ mm diameter, and with a near zero transverse velocity. The spatial overlap of such a molec-

ular beam with the thin (~ 150 μm) optical lattice results in about 4.1% of the molecules traversing a region in the optical field that contains a local minimum in the $|t\rangle$ state potential. The velocity acceptance, as is indicated by the green shaded (dotted) area in Figure 3a for the on-axis case, integrates to 1.4% of these molecules also having the right velocity to be captured. By taking into account that at best 75% of the molecules can make it to the $|t\rangle$ state, we estimate to capture $\sim 0.04\%$ of the incoming molecules. In the case of a Stark decelerated beam that delivers $\sim 2 \cdot 10^6$ molecules at 10 Hz [41], this results in ~ 880 trapped molecules per shot.

A possible improvement to the velocity acceptance may be realized by modulating the strength of the electric fields with time. In this dynamic scheme, which is illustrated in Figure 3b, we propose to use a pulsed molecular beam where the molecules are left to propagate freely for some time prior to entering the electric field gradient. By appropriately synchronizing the field strength with the arrival of the now temporally separated velocity components, we may effectively sweep larger parts of the velocity distribution into the optical trap. We expect the capture rate to potentially improve to about 1%, which is when the on-axis velocity capture efficiency is increased to one. Further investigation of this dynamic scheme could be done by simulating the molecular trajectories through the setup.

V. APPLICABILITY

Once the molecules are trapped, they can either be used directly to perform a (precision) measurement, or they can be transported using an optical conveyor belt. The latter can be achieved by designing the dipole trap using a ring type optical cavity, and by coupling two counter propagating laser beams whose frequencies are slightly detuned, effectively moving the trap minima at

a velocity that is proportional to the detuning. Performance experiments directly after capturing may be limited due to the presence of the static electric fields, but also photon scatterings due to the off-resonant trapping laser may become problematic at high intensities. In a far-off resonance trap, the scattering rate can be estimated through [67]

$$\gamma_{\text{scat}} \approx \frac{U \Gamma}{\hbar \Delta}, \quad (3)$$

where γ_{scat} represents the photon scattering rate, U the trap depth, Γ the linewidth of the transition, and Δ the detuning of the trapping light with that transition. For our case, we estimate $\gamma_{\text{scat}} = 5$ Hz. The scattering rate could be reduced by; 1) reducing the trap depth, which in turn increases the velocity sensitivity of the loading scheme. This results in fewer trapped molecules that would individually remain trapped for a longer time. Or 2) by increasing the detuning from the lowest allowed dipole transition. An increased detuning can primarily be achieved by replacing the trapping laser with a source that can produce light at a larger wavelength. The closest realisation of a conservative optical trap can be achieved using a CO₂ laser to produce light at a 10.6 μm wavelength. Such a quasi-electrostatic trap can reach scattering rates down to a 10 mHz regime, but it may also cause mixing of the $A^2\Pi$ states, which would be unfavorable for the loading scheme. It may also be possible to suppress certain electronic transitions by appropriately choosing the trap polarization. For instance, in BaF the lowest dipole allowed transition $X^2\Sigma \rightarrow A^2\Pi$ can be suppressed by using light that is polarized parallel to the quantisation axis.

An additional factor that limits the lifetime of the trapped molecules originates from the coupling of black-body radiation to the rovibrational transitions of the

molecule, as they may alter how the molecule interacts with the trap. Such rovibrational lifetimes for BaF were previously calculated to be 1.8 s at room temperature [68], and can be significantly improved by cooling down the surroundings of the molecule.

VI. CONCLUSION

In conclusion, we have outlined the main considerations needed to realise a single-photon loading scheme. The scheme makes use of the state-dependent potential in an inhomogeneous electric field. Using BaF as a prototype molecule, we have estimated the loading efficiency to be of the order $\sim 0.04\%$ for a typical Stark decelerated beam, which comes down to ~ 880 molecules per shot. The velocity-selective contribution to this efficiency can potentially be improved by a factor 20 when the external electric fields are synchronously modulated with the arrival time of different velocity components. The irreversibility of the loading process allows the accumulation of larger numbers of molecules over time, where the maximum accumulation number is limited by the trap lifetime. This single-photon loading scheme does not rely on optical cycling, which is beneficial for molecules that are difficult to laser cool. The ability to efficiently trap complex molecular species opens new opportunities to study cold molecular chemistry, quantum information, and fundamental interactions using optical traps.

ACKNOWLEDGMENTS

This research was made possible through funding from the Dutch Research Council (NWO) through grants XL21.074 and VI.C.212.016.

-
- [1] L. D. Carr, D. DeMille, R. V. Krems, and J. Ye, Cold and ultracold molecules: science, technology and applications, *New J. Phys.* **11**, 055049 (2009).
 - [2] R. V. Krems, Cold controlled chemistry, *Phys. Chem. Chem. Phys.* **10**, 4079 (2008).
 - [3] S. Ospelkaus, K.-K. Ni, D. Wang, M. H. G. d. Miranda, B. Neyenhuis, G. Quémener, P. S. Julienne, J. L. Bohn, D. S. Jin, and J. Ye, Quantum-State Controlled Chemical Reactions of Ultracold Potassium-Rubidium Molecules, *Science* **327**, 853 (2010).
 - [4] B. K. Stuhl, M. T. Hummon, and J. Ye, Cold State-Selected Molecular Collisions and Reactions, *Ann. Rev. Phys. Chem.* **65**, 501 (2014).
 - [5] B. Zhao and J.-W. Pan, Quantum control of reactions and collisions at ultralow temperatures, *Chem. Soc. Rev.* **51**, 1685 (2022).
 - [6] Y. Liu and K.-K. Ni, Bimolecular chemistry in the ultracold regime, *Ann. Rev. Phys. Chem.* **73**, 73 (2022).
 - [7] T. Karman, M. Tomza, and J. Pérez-Ríos, Ultracold chemistry as a testbed for few-body physics, *Nat. Phys.* **20**, 722 (2024).
 - [8] D. DeMille, Quantum Computation with Trapped Polar Molecules, *Phys. Rev. Lett.* **88**, 067901 (2002).
 - [9] S. L. Cornish, M. R. Tarbutt, and K. R. A. Hazzard, Quantum computation and quantum simulation with ultracold molecules, *Nat. Phys.* **20**, 730 (2024).
 - [10] V. Andreev, D. G. Ang, D. DeMille, J. M. Doyle, G. Gabrielse, J. Haefner, N. R. Hutzler, Z. Lasner, C. Meisenhelder, B. R. O’Leary, C. D. Panda, A. D. West, E. P. West, and X. Wu, Improved limit on the electric dipole moment of the electron, *Nature* **562**, 355 (2018).
 - [11] T. S. Roussy, L. Caldwell, T. Wright, W. B. Cairncross, Y. Shagam, K. B. Ng, N. Schlossberger, S. Y. Park, A. Wang, J. Ye, and E. A. Cornell, An improved bound on the electron’s electric dipole moment, *Science* **381**, 46 (2023).

- [12] E. S. Shuman, J. F. Barry, and D. DeMille, Laser cooling of a diatomic molecule, *Nature* **467**, 820 (2010).
- [13] M. T. Hummon, M. Yeo, B. K. Stuhl, A. L. Collopy, Y. Xia, and J. Ye, 2D Magneto-Optical Trapping of Diatomic Molecules, *Phys. Rev. Lett.* **110**, 143001 (2013).
- [14] V. Zhelyazkova, A. Cournol, T. E. Wall, A. Matsushima, J. J. Hudson, E. A. Hinds, M. R. Tarbutt, and B. E. Sauer, Laser cooling and slowing of CaF molecules, *Phys. Rev. A* **89**, 053416 (2014).
- [15] I. Kozryyev, L. Baum, K. Matsuda, B. L. Augenbraun, L. Anderegg, A. P. Sedlack, and J. M. Doyle, Sisyphus Laser Cooling of a Polyatomic Molecule, *Phys. Rev. Lett.* **118**, 173201 (2017).
- [16] S. Truppe, H. J. Williams, M. Hambach, L. Caldwell, N. J. Fitch, E. A. Hinds, B. E. Sauer, and M. R. Tarbutt, Molecules cooled below the Doppler limit, *Nat. Phys.* **13**, 1173 (2017).
- [17] J. Lim, J. R. Almond, M. A. Trigatzis, J. A. Devlin, N. J. Fitch, B. E. Sauer, M. R. Tarbutt, and E. A. Hinds, Laser Cooled YbF Molecules for Measuring the Electron's Electric Dipole Moment, *Phys. Rev. Lett.* **120**, 123201 (2018).
- [18] L. Anderegg, B. L. Augenbraun, Y. Bao, S. Burchesky, L. W. Cheuk, W. Ketterle, and J. M. Doyle, Laser cooling of optically trapped molecules, *Nat. Phys.* **14**, 890 (2018).
- [19] R. L. McNally, I. Kozryyev, S. Vazquez-Carson, K. Wenz, T. Wang, and T. Zelevinsky, Optical cycling, radiative deflection and laser cooling of barium monohydride ($^{138}\text{Ba}1\text{H}$), *New J. Phys.* **22**, 083047 (2020).
- [20] D. Mitra, N. B. Vilas, C. Hallas, L. Anderegg, B. L. Augenbraun, L. Baum, C. Miller, S. Raval, and J. M. Doyle, Direct laser cooling of a symmetric top molecule, *Science* **369**, 1366 (2020).
- [21] M. Rockenhäuser, F. Kogel, T. Garg, S. A. Morales-Ramírez, and T. Langen, Laser cooling of barium monofluoride molecules using synthesized optical spectra, *Phys. Rev. Res.* **6**, 043161 (2024).
- [22] J. Dai, Q. Sun, B. C. Riley, D. Mitra, and T. Zelevinsky, Laser cooling of a fermionic molecule, *Phys. Rev. Res.* **6**, 033135 (2024).
- [23] L. Anderegg, B. L. Augenbraun, E. Chae, B. Hemmerling, N. R. Hutzler, A. Ravi, A. Collopy, J. Ye, W. Ketterle, and J. M. Doyle, Radio Frequency Magneto-Optical Trapping of CaF with High Density, *Phys. Rev. Lett.* **119**, 103201 (2017).
- [24] A. L. Collopy, S. Ding, Y. Wu, I. A. Finneran, L. Anderegg, B. L. Augenbraun, J. M. Doyle, and J. Ye, 3D Magneto-Optical Trap of Yttrium Monoxide, *Phys. Rev. Lett.* **121**, 213201 (2018).
- [25] L. Baum, N. B. Vilas, C. Hallas, B. L. Augenbraun, S. Raval, D. Mitra, and J. M. Doyle, 1D Magneto-Optical Trap of Polyatomic Molecules, *Phys. Rev. Lett.* **124**, 133201 (2020).
- [26] N. B. Vilas, C. Hallas, L. Anderegg, P. Robichaud, A. Winnicki, D. Mitra, and J. M. Doyle, Magneto-optical trapping and sub-Doppler cooling of a polyatomic molecule, *Nature* **606**, 70 (2022).
- [27] J. J. Bureau, P. Aggarwal, K. Mehling, and J. Ye, Blue-Detuned Magneto-optical Trap of Molecules, *Phys. Rev. Lett.* **130**, 193401 (2023).
- [28] Z. Zeng, S. Deng, S. Yang, and B. Yan, Three-Dimensional Magneto-Optical Trapping of Barium Monofluoride, *Phys. Rev. Lett.* **133**, 143404 (2024).
- [29] S. J. Li, C. M. Holland, Y. Lu, and L. W. Cheuk, Blue-Detuned Magneto-optical Trap of CaF Molecules, *Phys. Rev. Lett.* **132**, 233402 (2024).
- [30] J. F. Barry, D. J. McCarron, E. B. Norrgard, M. H. Steinecker, and D. DeMille, Magneto-optical trapping of a diatomic molecule, *Nature* **512**, 286 (2014).
- [31] M. L. Wall, K. Maeda, and L. D. Carr, Realizing unconventional quantum magnetism with symmetric top molecules, *New J. Phys.* **17**, 025001 (2015).
- [32] L. D. Augustovičová and J. L. Bohn, Ultracold collisions of polyatomic molecules: CaOH, *New J. Phys.* **21**, 103022 (2019).
- [33] N. R. Hutzler, Polyatomic molecules as quantum sensors for fundamental physics, *Quantum Sci. Technol.* **5**, 044011 (2020).
- [34] R. Bause, N. Balasubramanian, T. Fikkers, E. H. Prinsen, K. Steinebach, A. Jadbabaie, N. R. Hutzler, I. A. Aucar, L. F. Pašteka, A. Borschevsky, and S. Hoekstra, Prospects for measuring the electron's electric dipole moment with polyatomic molecules in an optical lattice, *Physical Review A* **111**, 062815 (2025), 2411.00441.
- [35] G. N. Price, S. T. Bannerman, E. Narevicius, and Raizen, and M. G., Single-Photon Atomic Cooling, *Laser Phys.* **17**, 965 (2007).
- [36] E. Narevicius, S. T. Bannerman, and M. G. Raizen, Single-photon molecular cooling, *New J. Phys.* **11**, 055046 (2009).
- [37] A. M. Jayich, A. C. Vutha, M. T. Hummon, J. V. Porto, and W. C. Campbell, Continuous all-optical deceleration and single-photon cooling of molecular beams, *Phys. Rev. A* **89**, 023425 (2014).
- [38] G. N. Price, S. T. Bannerman, K. Viering, E. Narevicius, and M. G. Raizen, Single-Photon Atomic Cooling, *Phys. Rev. Lett.* **100**, 093004 (2008).
- [39] J. Riedel, S. Hoekstra, W. Jäger, J. J. Gilijamse, S. Y. T. v. d. Meerakker, and G. Meijer, Accumulation of Stark-decelerated NH molecules in a magnetic trap, *Eur. Phys. J. D* **65**, 161 (2011).
- [40] H.-I. Lu, I. Kozryyev, B. Hemmerling, J. Piskorski, and J. M. Doyle, Magnetic Trapping of Molecules via Optical Loading and Magnetic Slowing, *Phys. Rev. Lett.* **112**, 113006 (2014).
- [41] P. Aggarwal, H. L. Bethlem, A. Borschevsky, M. Denis, K. Esajas, P. A. B. Haase, Y. Hao, S. Hoekstra, K. Jungmann, T. B. Meijknecht, M. C. Mooij, R. G. E. Timmermans, W. Ubachs, L. Willmann, and A. Zapara, Measuring the electric dipole moment of the electron in BaF, *Eur. Phys. J. D* **72**, 197 (2018).
- [42] S. J. Li, H. D. Ramachandran, R. Anderson, and A. C. Vutha, Optical control of BaF molecules trapped in neon ice, *New J. Phys.* **25**, 082001 (2023).
- [43] A. Boeschoten, V. R. Marshall, T. B. Meijknecht, A. Touwen, H. L. Bethlem, A. Borschevsky, S. Hoekstra, J. W. F. v. Hofslot, K. Jungmann, M. C. Mooij, R. G. E. Timmermans, W. Ubachs, L. Willmann, and N.-m. x. w. o. Collaboration, Spin-precession method for sensitive electric dipole moment searches, *Phys. Rev. A* **110**, L010801 (2024).
- [44] Z. Corriveau, R. L. Lambo, D. Heinrich, J. P. Garcia, N. T. McCall, H. M. Yau, T. Chauhan, G. K. Koyanagi, A. Marsman, M. C. George, C. H. Storry, M. Horbatsch, and E. A. Hessels, Matrix isolated barium monofluoride: Assembling a sample of baf molecules for a measurement of the electron electric dipole moment (2024), [arXiv:2410.04591](https://arxiv.org/abs/2410.04591) [physics.atom-ph].

- [45] C. M. Western, Pghoper: A program for simulating rotational, vibrational and electronic spectra, *J. Quant. Spectrosc. Radiat. Transfer* **186**, 221 (2017).
- [46] C. Ryzlewicz and T. Törring, Formation and microwave spectrum of the 2Σ -radical barium-monofluoride, *Chemical Physics* **51**, 329 (1980).
- [47] W. E. Ernst, J. Kändler, and T. Törring, Hyperfine structure and electric dipole moment of BaF X $2\Sigma^+$, *The Journal of Chemical Physics* **84**, 4769 (1986).
- [48] F. L. Kien, P. Schneeweiss, and A. Rauschenbeutel, Dynamical polarizability of atoms in arbitrary light fields: general theory and application to cesium, *Eur. Phys. J. D* **67**, 92 (2013).
- [49] L. Caldwell and M. R. Tarbutt, Sideband cooling of molecules in optical traps, *Phys. Rev. Res.* **2**, 013251 (2020).
- [50] T. Saue *et al.*, The DIRAC Code for Relativistic Molecular Calculations, *J. Chem. Phys.* **152**, 204104 (2020).
- [51] DIRAC, a relativistic ab initio electronic structure program, Release DIRAC23 (2023), written by A. S. P. Gomes *et al.* (available at <https://doi.org/10.5281/zenodo.7670749>, see also <http://www.diracprogram.org>).
- [52] U. Kaldor, The Fock space coupled cluster method: theory and application, *Theoret. Chim. Acta* **80**, 427 (1991).
- [53] M. Iliáš and T. Saue, An infinite-order two-component relativistic Hamiltonian by a simple one-step transformation, *J. Chem. Phys.* **126**, 064102 (2007).
- [54] K. G. Dyall, Relativistic double-zeta, triple-zeta, and quadruple-zeta basis sets for the 4s, 5s, 6s, and 7s elements, *J. Phys. Chem. A* **113**, 12638 (2009).
- [55] K. G. Dyall, Relativistic double-zeta, triple-zeta, and quadruple-zeta basis sets for the light elements h–ar, *Theor. Chem. Acc.* **135**, 128 (2016).
- [56] D. A. Matthews, L. Cheng, M. E. Harding, F. Lipparini, S. Stopkowicz, T.-C. Jagau, P. G. Szalay, J. Gauss, and J. F. Stanton, Coupled-Cluster Techniques for Computational Chemistry: The CFOUR Program Package, *J. Chem. Phys.* **152**, 214108 (2020).
- [57] J. F. Stanton, J. Gauss, L. Cheng, M. E. Harding, D. A. Matthews, and P. G. Szalay, CFOUR, Coupled-Cluster Techniques for Computational Chemistry, a Quantum-Chemical Program Package, For the current version, see <http://www.cfour.de>.
- [58] R. A. Kendall, T. H. Dunning, and R. J. Harrison, Electron affinities of the first-row atoms revisited. Systematic basis sets and wave functions, *The Journal of Chemical Physics* **96**, 6796–6806 (1992).
- [59] I. S. Lim, H. Stoll, and P. Schwerdtfeger, Relativistic small-core energy-consistent pseudopotentials for the alkaline-earth elements from Ca to Ra, *J. Chem. Phys.* **124**, 034107 (2006).
- [60] J. G. Hill and K. A. Peterson, Gaussian basis sets for use in correlated molecular calculations. xi. pseudopotential-based and all-electron relativistic basis sets for alkali metal (K–Fr) and alkaline earth (Ca–Ra) elements, *J. Chem. Phys.* **147**, 244106 (2017).
- [61] E. H. Prinsen, I. A. Aucar, S. Hoekstra, A. Borschevsky, and L. F. Pašteka, (2025), in preparation.
- [62] H. L. Bethlem, M. R. Tarbutt, J. K?pper, D. Carty, K. Wohlfart, E. A. Hinds, and G. Meijer, Alternating gradient focusing and deceleration of polar molecules, *Journal of Physics B: Atomic, Molecular and Optical Physics* **39**, R263 (2006), physics/0604020.
- [63] K. Wohlfart, F. Filsinger, F. Grätz, J. Küpper, and G. Meijer, Stark deceleration of OH radicals in low-field-seeking and high-field-seeking quantum states, *Physical Review A* **78**, 033421 (2008), 0807.4022.
- [64] Y. Hao, L. F. Pašteka, L. Visscher, t. N.-e. collaboration, :, P. Aggarwal, H. L. Bethlem, A. Boeschoten, A. Borschevsky, M. Denis, K. Esajas, S. Hoekstra, K. Jungmann, V. R. Marshall, T. B. Meijknecht, M. C. Mooij, R. G. E. Timmermans, A. Touwen, W. Ubachs, L. Willmann, Y. Yin, and A. Zapara, High accuracy theoretical investigations of CaF, SrF, and BaF and implications for laser-cooling, *J. Chem. Phys.* **151**, 034302 (2019).
- [65] P. Aggarwal, V. R. Marshall, H. L. Bethlem, A. Boeschoten, A. Borschevsky, M. Denis, K. Esajas, Y. Hao, S. Hoekstra, K. Jungmann, T. B. Meijknecht, M. C. Mooij, R. G. E. Timmermans, A. Touwen, W. Ubachs, S. M. Vermeulen, L. Willmann, Y. Yin, A. Zapara, and N.-e. Collaboration, Lifetime measurements of the A $2\Pi_{1/2}$ and A $2\Pi_{3/2}$ states in BaF, *Phys. Rev. A* **100**, 052503 (2019).
- [66] T. Chen, W. Bu, and B. Yan, Structure, branching ratios, and a laser-cooling scheme for the BaF138 molecule, *Phys. Rev. A* **94**, 063415 (2016).
- [67] R. Grimm, M. Weidemüller, and Y. B. Ovchinnikov, Optical dipole traps for neutral atoms (Academic Press, 2000) pp. 95–170.
- [68] S. Y. Buhmann, M. R. Tarbutt, S. Scheel, and E. A. Hinds, Surface-induced heating of cold polar molecules, *Physical Review A* **78**, 052901 (2008), 0806.2913.